AD-A123 480 EXPERIMENTAL DETERMINATION OF TWO-PHOTON AND OTHER NONLINEAR ABSORPTION I..(U) HARVARD UNIV CAMBRIDGE MASS DIV OF ENGINEERING AND APPLIED PH.. 1/1

UNCLASSIFIED N BLOEMBERGEN ET AL. 31 MAR 77 F/G 20/6 NL

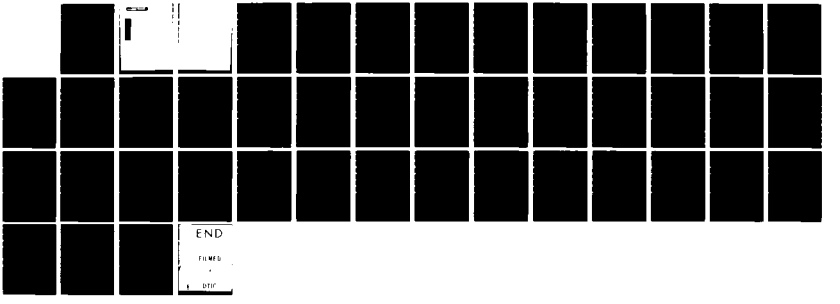

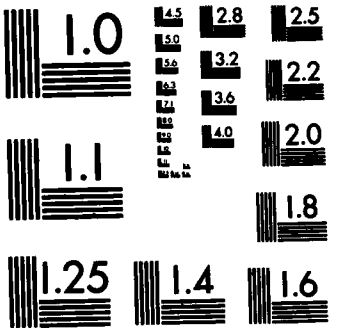

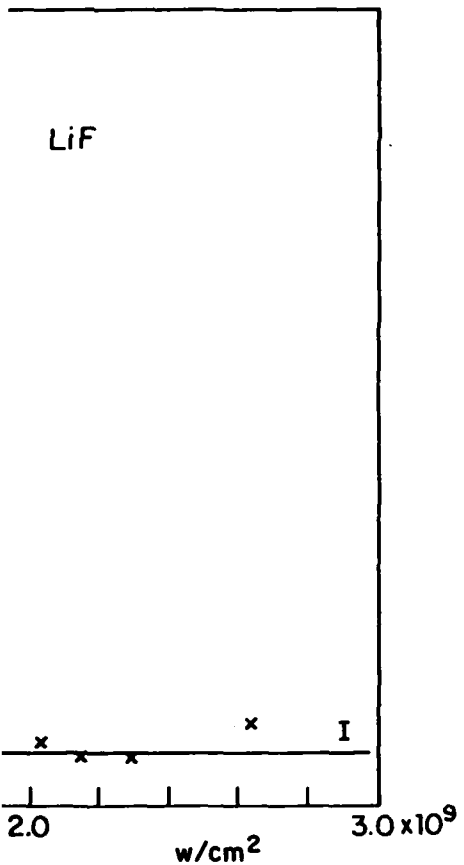

Unclassified

SECURITY CLASSIFICATION OF THIS PAGE *(When Data Entered)*

REPORT DOCUMENTATION PAGE		READ INSTRUCTIONS BEFORE COMPLETING FORM
1. REPORT NUMBER Semiannual Technical Report	2. GOVT ACCESSION NO.	3. RECIPIENT'S CATALOG NUMBER
4. TITLE *(and Subtitle)* EXPERIMENTAL DETERMINATION OF TWO-PHOTON AND OTHER NONLINEAR ABSORPTION IN ULTRAVIOLET AND INFRARED WINDOW MATERIALS		5. TYPE OF REPORT & PERIOD COVERED Semiannual Technical Report, 10-1-76 - 3-31-77 6. PERFORMING ORG. REPORT NUMBER
7. AUTHOR(s) N. Bloembergen J. Blake		8. CONTRACT OR GRANT NUMBER(s) ARPA Contract F44620-75-C-0088
9. PERFORMING ORGANIZATION NAME AND ADDRESS Division of Engineering and Applied Physics Harvard University Cambridge, Mass. 02138		10. PROGRAM ELEMENT, PROJECT, TASK AREA & WORK UNIT NUMBERS
11. CONTROLLING OFFICE NAME AND ADDRESS Advanced Research Projects Agency (DOD) 1400 Wilson Boulevard Arlington, Virginia 22209		12. REPORT DATE 10-1-76 to 3-31-77 13. NUMBER OF PAGES 40
14. MONITORING AGENCY NAME & ADDRESS*(if different from Controlling Office)* Air Force Office of Scientific Research Bolling Air Force Base Washington, D.C. 20332		15. SECURITY CLASS. *(of this report)* unclassified 15a. DECLASSIFICATION/DOWNGRADING SCHEDULE

16. DISTRIBUTION STATEMENT *(of this Report)*

APPROVED FOR PUBLIC RELEASE
DISTRIBUTION UNLIMITED

17. DISTRIBUTION STATEMENT *(of the abstract entered in Block 20, if different from Report)*

18. SUPPLEMENTARY NOTES

"This research was supported by the Advanced Research Projects Agency of the Department of Defense and was monitored by the Air Force Office of Scientific Research under Contract No. F44620-75-C-0088."

19. KEY WORDS *(Continue on reverse side if necessary and identify by block number)*

Alkali halides
Indium Antimonides
Infrared window absorption
Nonlinear absorption
Two-photon absorption cross sections
Ultraviolet window absorption
Window materials

20. ABSTRACT *(Continue on reverse side if necessary and identify by block number)*

Experimental determination of the two photon absorption cross section in a variety of window materials is carried out with picosecond harmonic pulses from a mode-locked Nd-YAG laser system, with nanosecond pulses from a combined ruby-dye laser system, and with subnanosecond CO_2-laser pulses. The measurements at 10 μm concentrate on the properties of the conduction and valence band of InSb. The measurements of the two photon absorption cross section in the near and far ultraviolet have covered a series of alkali halides, and will be extended to other fluoride and oxide UV window materials.

DD FORM 1 JAN 73 1473 EDITION OF 1 NOV 65 IS OBSOLETE

Unclassified

SECURITY CLASSIFICATION OF THIS PAGE *(When Data Entered)*

PREFACE

This semiannual technical report describes the work, performed under Contract Number F 44620-75-C-0088 at Harvard University, during the period October 1, 1976 - March 31, 1977.

The following investigators contributed to the report:

Professor N. Bloembergen, Principal Investigator

Professor E. Yablonovitch, Research Group Leader

Dr. H. Lotem, Research Fellow

Dr. C. de Araujo, Research Fellow

Mr. H.S. Kwok, Graduate Student

Mr. P. Liu, Graduate Student

Material in previous reports (see, for example, Cruft Laboratory Technical Report 665, October 1976), is not duplicated.

The views and conclusions contained in this document are those of the authors and should not be interpreted as necessarily representing the official policies, either expressed or implied, of the Defense Advanced Research Projects Agency or the U.S. Government.

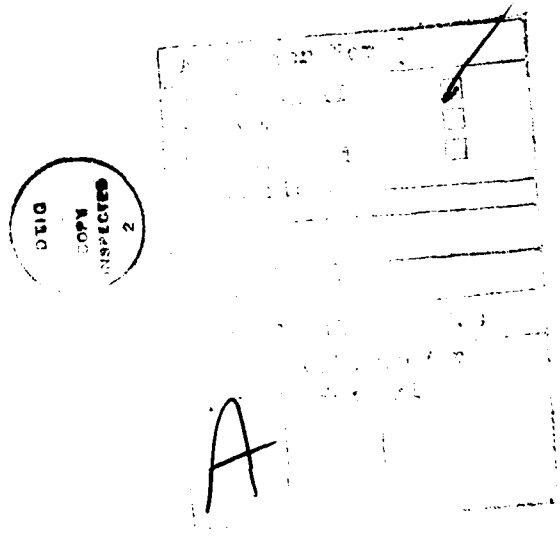

A. REPORT SUMMARY

High power excimer lasers operating in the ultraviolet region of the spectrum have revealed limitations imposed by failure of window materials and coatings. More reliable, quantitative data on two photon absorption cross sections and other nonlinear processes in ultraviolet window and coating materials are needed.

We have developed at Harvard University over the past several years, various techniques to study quantitatively breakdown thresholds and other nonlinear phenomena. Reproducible single picosecond pulses with Gaussian temporal and spatial profiles are available from a Nd-Yag system. We have used pulses at the fourth harmonic frequency, corresponding to the ultraviolet wave length $\lambda = 266$ nm, to measure the two-photon absorption cross section in a number of alkali halide crystals. The results are detailed in Section B of this report. The intrinsic two-photon absorption coefficients lie in the range $1 - 4\times10^{-3}$ cm/Mega watt. Details may be found in Table 1 of Section B. The cross sections appear to be about one order of magnitude smaller than previously reported for KCl and RbBr. Lithium fluoride with a bandgap larger than $2\hbar\omega$, does not show any detectable two-photon absorption at 266 nm. The data will be extended to other wavelengths, notably the third harmonic at 355 nm, and to other oxide and fluoride window and coating materials.

A ruby laser system, coupled with a dye laser pumped by the second harmonic pulse of the ruby frequency, has been used to measure the two-photon absorption cross section in TiO_2, GaP, CdS and $SrTiO_3$. A novel method has been developed, in which the two photon absorption cross section is compared with known attenuation due to the inverse

raman effect in cyclohexane. Details are described in Section C of this report, which is essentially a manuscript submitted for publication in the Physical Review. This work will be extended to higher frequencies and materials with wider bandgaps. It would be of particular interest to vary the dye laser frequency, so that the two photon absorption cross section can be scanned across the intrinsic band gap.

Finally, the nonlinear infrared absorption in InSb is being studied. The subnanosecond CO_2-pulsed laser facility permits the study of nonlinear effects, at intensity, which in longer pulses would invariably damage the window material. The intrinsic distortion of valence and conduction band in InSb has been studied theoretically by others, notably Tsoar and Gersten. A nonlinear behavior of the transmittance and reflectance of InSb during the short pulses has been observed. These data are presented in Section D of this report. Their interpretation in terms of solid state plasma theory is continuing.

B. TWO-PHOTON ABSORPTION OF ALKALI-HALIDES AT 266 nm

Due to the increasing interest in u.v. lasers, it will be useful to know the absolute value of absorption coefficients of materials with large band gap like Alkali-halides which have band gap range from 5.6 eV to 12.5 eV. Few data were published for Alkali-bromides and Alkali-iodides [1-4]. In this experiment the absorption of Alkali-halides were studied with the 4-th harmonic of YAG-Nd laser at 266 nm.

The Alkali-halides can absorb the 266 nm photon (4.66 eV) appreciably through nonlinear processes at high intensity. The two photon transition rate $W^{(2)}$ is given by second order perturbation theory [5-6], and Keldysh model [7].

The method used is described elsewhere [8]. The attenuation of the beam is given by

$$\frac{dI}{dz} = -\alpha I - \beta I^2 \quad . \tag{1}$$

α is the one-photon absorption coefficient, and β is the two photon absorption coefficient, which is related to $W^{(2)}$ by

$$\beta = 2\hbar\omega \frac{W^{(2)}}{I^2} \tag{2}$$

The transmitted intensity can be found from (1)

$$I(r,\ell,t) = \frac{(1-R)^2 I(r,\ell,t)\, e^{-\alpha \ell}}{1+\beta(1-R)I(r,\ell,t)(1-e^{-\alpha \ell})/\alpha} \tag{3}$$

where ℓ is the thickness of the sample. R is the surface reflectivity the multiple reflection within the medium is neglected.

The mode-locked YAG-Nd laser-amplifier system is described in [8] and in a previous joint technical report (ARPA and Joint Services Electronic Program No. 665, October 1976). The system gives a 10 mJ single pulse at 1.06 μm. The beam profile was measured carefully. It is Gaussian both in space and time. The pulse has duration 30 ps. at full width half maximum. The fundamental is frequency doubled by CDA crystal, then doubled again by ADP crystal (Fig. 1). Both are temperature tuned 90° phase matching which gives no walk-off. The overall power conversion efficiency at 100 MW input is 20%. The beam profile at 266 nm is monitored by photo-diode array, and fitted with a Gaussian curve with 1/e radius 0.68 mm.

In order to give absolute values, the beam is monitored carefully. A plane vacuum photo-diode D_1 (Fig. 1) is used with fast oscilloscope to make sure the beam is a single pulse. The fluctuation in the pulse width is taken into account by monitoring the energy of each pulse both at 1.06 μm and 266 nm [9]. Consider the fundamental Gaussian pulse as

$$I(r,t) = I_m e^{-(r/d)^2} \cdot e^{-(t/\tau)^2} \quad . \tag{4}$$

The energy is given by $E_f = \pi^{1/2} I_m \tau A$, where $A = \pi d^2$. The 4-th harmonic has energy $E_h = q\pi^{1/2} I_m^4 \tau' A'$ where $\tau' = \tau/2$, $A' = A/4$, and q is the conversion efficiency. We have

$$\left(\frac{E_f^4}{E_h}\right)^{1/3} \propto \tau A \quad . \tag{5}$$

The intensity at the sample is increased by a pair of focusing-collimating lenses. The sample is put behind the focus to avoid self-focusing. The focal length of the lens is measured by comparing the

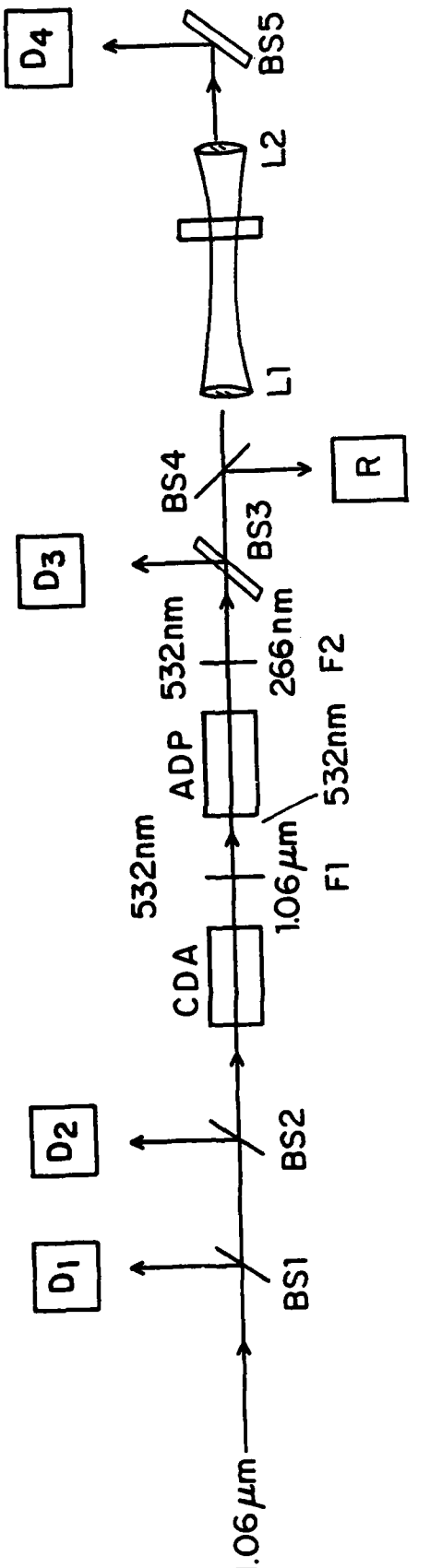

FIG. 1 BS. BEAM SPLITTERS D. PHOTODIODES F. FILTERS L. LENSES
R. RETICON PHOTODIODE ARRAY.

beam sizes before and after the lenses system. With a photo-diode array, the focal length is determined to be 24.7 ± 0.3 cm.

In order to determine β, the energy transmission coefficient is measured. For a Gaussian beam:

$$I(r,\ell,t) = \frac{I_m e^{-(r/d)^2} e^{-(t/\tau)^2} (1-R)^2 e^{-\alpha\ell}}{1 + \beta I_m (1-R) e^{-(r/d)^2} e^{-(t/\tau)^2} (1-e^{-\alpha\ell})/\alpha} \tag{6}$$

$$T = \frac{E^{out}}{E^{in}} = \frac{2\pi \int_0^\infty r dr \int_{-\infty}^\infty I_m(r,\ell,t)\, dt}{I_m \pi d^2 \pi^{1/2} \tau}$$

$$= 2\frac{\alpha}{\beta} \cdot \frac{e^{-\alpha\ell}}{I_m \pi^{1/2}} \cdot \frac{1-R}{1-e^{-\alpha\ell}} \int_0^\infty \ln\left(1 + \frac{\beta}{\alpha} I_m (1-R)(1-e^{-\alpha\ell}) e^{-x^2}\right) \tag{7}$$

At low intensity, we can get an approximate form for the integration. We find:

$$\lim_{I_m \to 0} T \cong e^{-\alpha\ell}(1-R)^2 \tag{8}$$

$$\lim_{I_m \to 0} \frac{d(1/T)}{d I_m} \cong \frac{\beta}{\alpha} \frac{(1-e^{-\alpha\ell})}{2\sqrt{2}\,(1-R)e^{-\alpha\ell}} \tag{9}$$

The approximation is good for $(\beta/\alpha) I_m (1-R)(1-e^{-\alpha\ell}) < 1$, which is true in the experiment for I_m as large as $600\ MW/cm^2$. Also, the one-photon absorption coefficient α is small in Alkali-halides. We get

$$\lim_{I_m \to 0} T \simeq (1-R)^2 \tag{10}$$

$$\lim_{I_m \to 0} \frac{d(1/T)}{d I_m} \simeq \frac{\beta \ell}{2\sqrt{2}(1-R)} \qquad (11)$$

Now, it is clear that the slope in $1/T$ verses I_m graph will give the β value.

I_m is measured with D_3 which is calibrated with respect to a thermocouple with calibration accuracy $\pm$ 5%.

Typical data is shown in Fig. 2. The rather large absorption at low intensity can be ascribed to surface polishing. From the approximate value of β found by Equation (11), a set of curves are generated by Equation (7) with different values of β near that approximate value. The β is then chosen by the best fit.

In order to make sure there is no artifact, the transmission coefficients are measured without sample and with sample having band gaps larger than $2\hbar\omega$. Typical data for LiF are shown in Fig. 3.

The error involved in the determination of β is found to be 8% from beam size, 12% from the approximation of constant conversion efficiency g which is intensity dependent [10], 5% from calibration of photodiode, and the scattering of data points which is 15% to 30%. Thus, the uncertainty is 40% - 55%.

Fluorescence is observed in the medium along the path of the beam [11, 12]. Visible color can be seen after a few shots. In KCl the absorption of 532 nm by the color track is observed which can be explained by the position of absorption band of F-center [13].

The physical process involved seems to be electron hole pairs generated by two-photon excitation. They form excitons and give out fluorescence. The exciton energy is given up to form Cl_2^- and F-center [14].

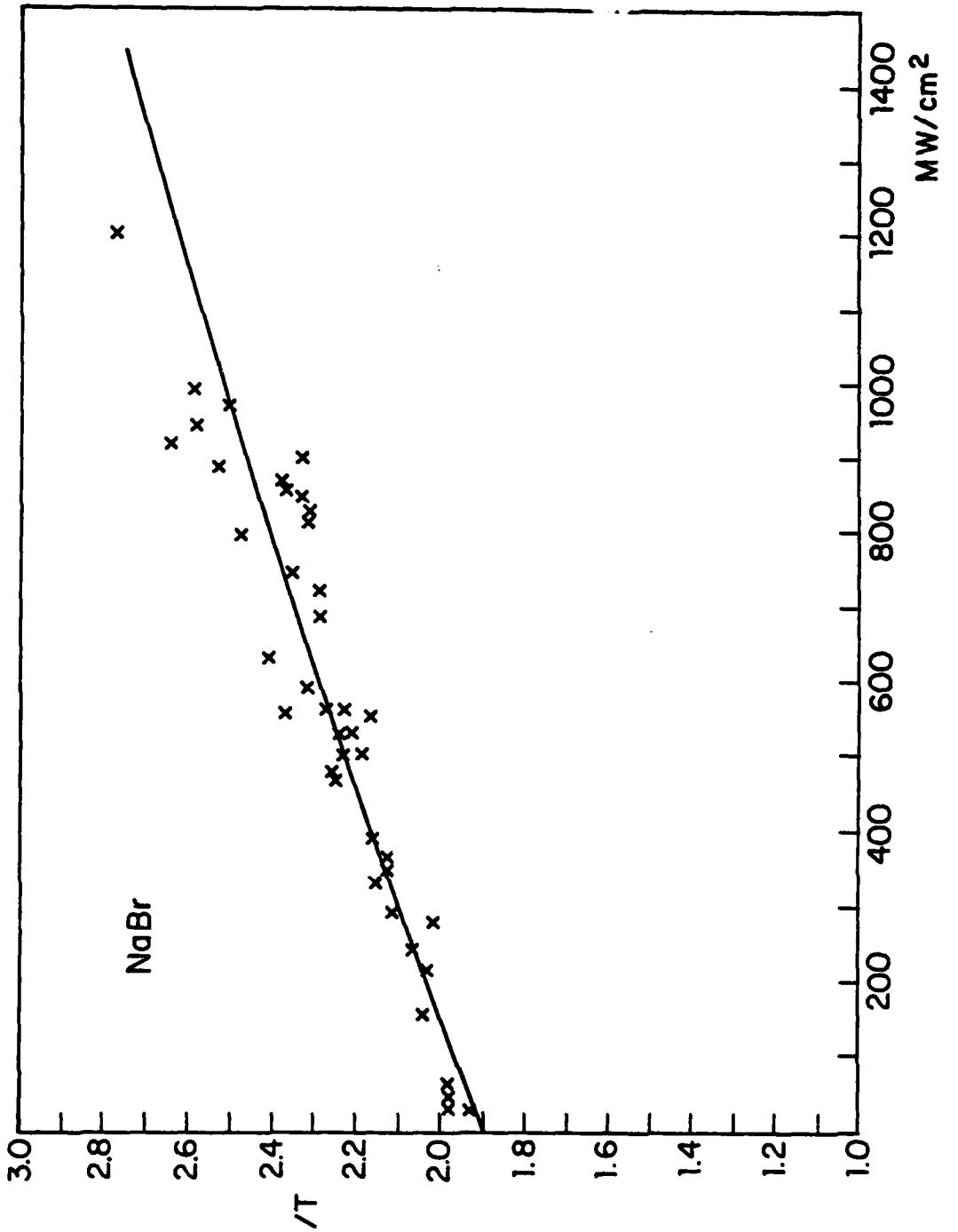
NaBr
1/T
3.0
2.8
2.6
2.4
2.2
2.0
1.8
1.6
1.4
1.2
1.0
200
400
600
800
1000
1200
1400
MW/cm²

FIGURE 2

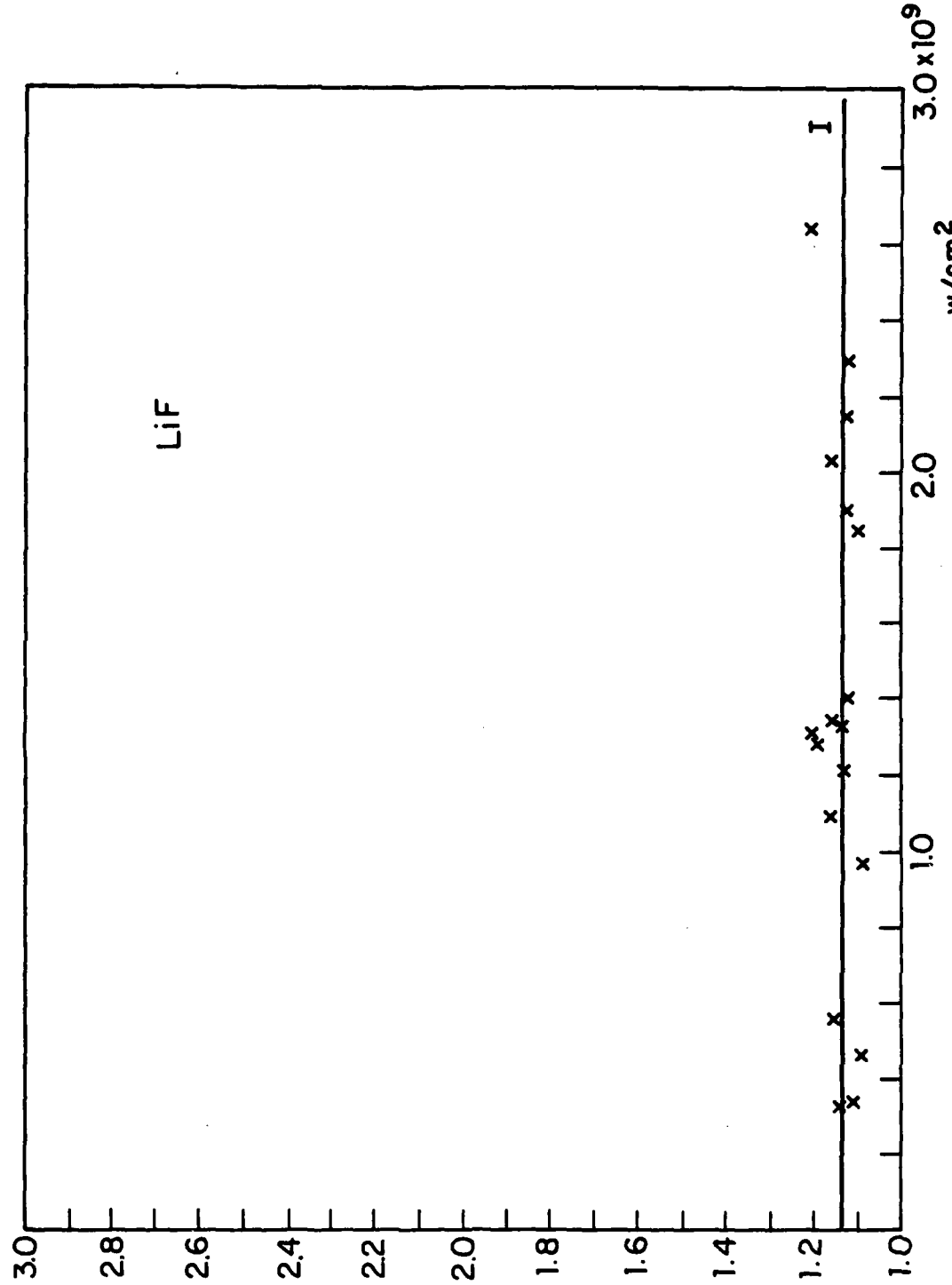

FIGURE 3

By measuring the transmission after the F-centers are formed and relaxed, it is found that there is no change in the two photon absorption coefficient. In order to determine any possible absorption other than two-photon absorption within the laser pulse, a better detection system to reduce the scattering of data points is needed.

The polarization dependence in KCl has been measured. A change of 50% is observed by changing the electric field from [001] to [011] direction.

Since the power used is much higher than the critical power for self-focusing [15], it is important to notice any change in beam size by self-focusing. The beam sizes before and after the sample are compared, and the measurements have been done with different sample thickness, also by observing the stable color track formed in U-center doped KCl [16] under a microscope. No evidence of self-focusing has been observed so far. It is possible that n_2 is changed by the two-photon absorbing levels, and self-focusing tends to concentrate the power while two-photon absorption tends to remove the power at the peak.

An electronic system to monitor the energy of laser pulse has been constructed, but noise from the spark gap in pockel cell single pulse selector presents a problem.

Numerical data for the two photon absorption coefficients in several alkali halides are listed in Table 1. These should be compared with earlier data listed in Table 2 but obtained by less accurate techniques available a decade ago. These were also quoted in the Eighth Technical Report, December 1976, by M. Sparks and C. J. Duthler of Xonics, Inc. It is seen that the intrinsic two photon absorption coefficients appear to be about one order of magnitude smaller.

Material	Eg (eV)	Surface Normal	$\vec{E}$	Par (KW)	ℓ (cm)	β cm/MW	Δ
NaCℓ	8.7	[100]	[001]	16	0.74	$3.5\times10^{-3}\pm 50\%$	$\simeq 4.7\times10^{-3}$ Keldysh
NaBr	7.7	[100]	[001]	8	0.74	$2.5\times10^{-3}\pm 40\%$	
KCℓ	8.5	[100]	[001]	20	0.74	$1.7\times10^{-3}\pm 45\%$	2.36×10^{-3} Ref. 16
KCℓ	8.5	[100]	[011]	20	0.74	$3.4\times10^{-3}\pm 50\%$	
KCℓ (F-centers)	8.5	[100]	[001]	20	0.74	$1.8\times10^{-3}\pm 55\%$	
KCℓ	8.5	[100]	[001]	20	2.10	$2.7\times10^{-3}\pm 55\%$	
RbCℓ	8.6	[100]	[001]	20	0.60	$1.02\times10^{-3}\pm 40\%$	
RbCℓ	8.6	[100]	[001]	20	1.91	$1.26\times10^{-3}\pm 55\%$	
RbBr	5.6	[100]	[001]	20	1.0	$2.18\times10^{-3}\pm 45\%$	
RbI	6.1	[100]	[001]	20	1.0	$2.49\times10^{-3}\pm 45\%$	
LiF	10.3	[100]	[001]	60	0.47	0	

TABLE 1

Material	Eg (eV)	E_1+E_2 (eV)	β (cm/MW)	Reference
RbI	6.26	7.0	2.07×10^{-2}	D. Frölich, P.R.L. 19, 496 (1967).
RbBr	7.25	8.0	1.23×10^{-2}	ibid.
KBr	7.4	8.0	1.30×10^{-2}	ibid.
KI		7.3	2.29×10^{-2}	K. Park, P.R.L. 22, 1426 (1968).
KI		4.7	7.5×10^{-3}	K. Park, P.R.L. 11, 414 (1963).
KI		4.59	7.58×10^{-3}	K. Park, P.R. 137, A1455 (1965).
CsBr		8.0	2.03×10^{-2}	D. Frölich, Phy. Stat. Sol. 40, 547 (1970).
CsI		7.1	4.11×10^{-2} (low temp.)	ibid.

General behavior

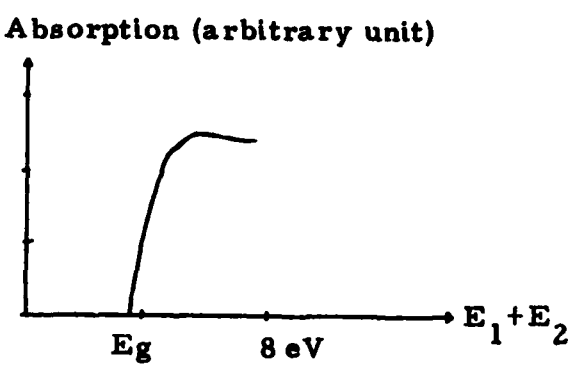

TABLE 2

It is planned to extend the measurements of the two photon absorption cross sections to other materials used in UV windows and coatings. Furthermore, data at the third harmonic of Nd-Yag at 353 nm will be taken.

References

1. K. Park, J. Hopfield, and J. Worlock, Phys. Rev. Lett. 11, 414 (1963).
2. K. Park et al., Phys. Rev. 137, A1455 (1965).
3. D. Frölich et al., Phys. Rev. Lett. 19, 496 (1967).
4. K. Part et al., Phys. Rev. Lett. 22, 1426 (1969).
5. H. Mahr, Two photon absorption spectroscopy, in Quantum Electronics edited by C.L. Tang.
6. J. Worlock, Two photon spectroscopy, in Laser Handbook, edited by F.T. Arecthi and E.O. Schulz-Du Bois.
7. L.V. Keldysh, Soviet Phys. JETP 20, 1307 (1965).
8. J.H. Bechtel and W.L. Smith, Phys. Rev. B 13, 3515 (1976).
9. J.H. Bechtel and W.L. Smith, Phys. Lett. 55A, 203 (1975).
10. D.R. White, E.L. Dawes, and J.H. Marburger, J. of Quantum Electronics QE-6, No. 12, 793 (1970).
11. M. Goller, D.E. Altman, and T.A. DeTemple, App. Phys. Lett. 11, 221 (1967).
12. J.N. Bradford, R.T. Williams, and W.L. Faust, Phys. Rev. Lett. 35, 300 (1976).
13. W.B. Fowler, Physics of Color Centers, edited by W.B. Fowler (Academic Press, New York, 1968).
14. Y. Toyozawa, Exciton lattice interaction--fluctuation, relaxation, and defects formation, in Proceedings of the IV International Conference on Vacuum Ultraviolet Radiation Physics, edited by E.E. Koch et al. (Pergamon, Vieweg, Hamburg, 1974).

15. S.A. Akhmanov et al., Self-focusing, self-defocusing and self-modulation of laser beams, in Laser Handbook.

16. L.F. Mollenauer et al., Phys. Rev. Lett. 35, 1662 (1975).

C. ABSOLUTE DETERMINATION OF THE TWO-PHOTON ABSORPTION COEFFICIENT RELATIVE TO THE INVERSE RAMAN CROSS SECTION

With the development of high-power lasers, it has become possible to investigate many nonlinear (NL) optical processes. In particular, the two-photon absorption (TPA) process by which two photons are simultaneously absorbed has been explored extensively. The selection rules for the TPA transitions are in general different from those of the one-photon transitions, and therefore, the measurement of the TPA properties of a material system is complementary to the linear measurements. A lot of information on the symmetry of the material eigenstates, including states which are unseen in linear spectroscopy, may be obtained from the relative values of the different components of the TPA tensor.[1] Information about the magnitude of the transition matrix elements, the density of states and the energy eigenvalues may be obtained from absolute measurements of the TPA coefficient and especially from its frequency dependence.[2] Unfortunately, these latter measurements are known to be difficult because of the strong dependence of the TPA process on the parameters of the lasers used. This fact is reflected by the large scattering of the reported results in the literature.[2]

New techniques for absolute measurement of the TPA coefficient have been recently reported.[3-9] In the first kind of technique, the value obtained for the TPA coefficient is based on a good knowledge of the laser's parameters.[3,4] These measurements can be performed only with those particular lasers which may be quite well characterized, and therefore the spectral region of the measurement is very limited. The second kind of technique, which is independent of the laser parameters, is based on absolute calibration of the TPA coefficient by other known nonlinear (NL)

cross sections. This type of measurement may be carried out at different laser frequencies. This was done in Ref. 5 using the second order NL susceptibility of quartz as the NL reference. A disadvantage of this specific calibration is the assumption that the quantum efficiency for the induced fluorescence by the absorption of one photon at 2ω is identical with the efficiency associated with TPA of two photons at ω. In Refs. 6-9 the calibration of the TPA cross-section is done in relation to well known Raman scattering cross sections. In contrast with all the other classical TPA techniques, this measurement, which utilizes a NL parametric mixing technique, is not associated with real material transitions and therefore stepwise multiphoton transitions do not interfere in the measurement[7] and the value for the TPA coefficient may be unambiguously obtained. Another simple normalization technique has been proposed recently[10] which is very useful for obtaining relative values of TPA coefficients of different materials independent of the properties of the laser used.[11] This method may give absolute TPA coefficients by using reference materials whose TPA coefficients have been measured by, for example, the method of Ref. 7.

The purpose of this paper is to report on a new method for the direct calibration of the TPA coefficient relative to well known inverse Raman cross sections.[8, 12, 13] By this method we calibrated the TPA of CdS, GaP, $SrTiO_3$ and TiO_2 at 31660 cm^{-1} relative to the Raman cross section of the strong 2855 cm^{-1} CH mode of liquid cyclohexane. Moreover, the dependence of the measurement on the laser parameters could be eliminated in a two-channel normalization experiment in ways similar to those used in Ref. 10, and thus very accurate and reliable TPA coefficients were

obtained. This general method may also be used for the calibration of absolute Raman cross sections.

Theory

When two laser beams, a strong beam at ω_L and a weaker probe beam at ω_P interact in a NL material system, the strong beam induces a change in the complex refractive index at the probe frequency. The real part of this change is proportional to $n^{(2)}$, the self-focussing coefficient,[14,15] while the imaginary part of this change is responsible for NL loss or gain at ω_P.[14] The net gain or loss at ω_P is proportional to the imaginary part of the NL third order susceptibility $\chi^{(3)}(-\omega_P, \omega_P, \omega_L, -\omega_L)$. Neglecting higher order processes, the probe intensity may be described by:[4]

$$\frac{dI_P}{dz} = -\alpha_P I_P - \beta I_L I_P \tag{1a}$$

where

$$\beta = 32\pi^2 \omega_P/(c^2 n_P n_L) \operatorname{Im} \chi^{(3)}(-\omega_P, \omega_P, \omega_L, -\omega_L) \ , \tag{1b}$$

I_i and n_i $(i = P, L)$ are the laser intensities and the refractive indices, at ω_P and ω_L, respectively, α_P is the linear absorption coefficient at ω_P, and c is the speed of light.

It is clear from Eqs. (1) that the NL process is enhanced whenever $\chi^{(3)}$ reaches a resonance.[16] We are dealing here with systems which are transparent at both ω_L and ω_P, and therefore only the resonances of $\chi^{(3)}$ which are associated with two-photon transitions (i.e., TPA or Raman)

of the material system will be taken into account. For a system occupying the ground state, loss at ω_P (or a positive contribution to $\mathrm{Im}\chi^{(3)}$) occurs in the TPA case, i.e., when $\omega_P + \omega_L$ is close to two-photon transitions of the material. Raman transitions, however, may contribute to both gain and loss at ω_P. When $\omega_L - \omega_P$ is close to a Raman transition, and $\omega_L > \omega_P$, the Raman contribution to $\mathrm{Im}\chi^{(3)}$ is negative and is associated with gain. This gain is responsible for the strong amplification in the stimulated Raman effect.[17] When $\omega_P > \omega_L$, the sign of the Raman contribution to $\mathrm{Im}\chi^{(3)}$ is positive and the Raman transition is associated with absorption at ω_P. The latter process, which is usually called the inverse Raman effect,[13, 8, 16] is used in this work for the absolute calibration of the TPA coefficients. The cross section of the inverse Raman effect is a measurable quantity since it is directly proportional to the spontaneous Raman cross section.

We will now explain the details of the calibration procedure. We first solve Eq. (1) for a slab of NL material of thickness d and get for the transmitted energy:

$$I_P(x, y, z = d, t) = (1-R_P)^2 I_P(x, y, z=0,\ t-n_P\, d/c) \times$$

$$\exp - \{\alpha_P\, d + \beta_{eff} I_L(x, y, z = 0, t-n_L\, d/c)\} \qquad (2)$$

$$\beta_{eff} = (1-R_L)\ (1-e^{-\alpha_L d})\ \beta/\alpha_L\ ,$$

where β is the TPA coefficient or the inverse Raman absorption coefficient and α_i, R_i and n_i $(i=P, L)$ are the one-photon absorption coefficients, the reflectance and the refractive indices, respectively. In the solution (2) we assume that only linear attenuation, and no back reflection,

affects the strong beam at ω_L. The total transmitted energy of the probe pulse, E_T, is given by the integration of I_P over the pulse duration and the pulse cross section. Neglecting the dispersion of the refractive index, which is a good assumption for long pulses and thin samples, we get for E_T:

$$E_T = \exp\{-\alpha_P d\}(1-R_P)^2 \iiint d\tau\, dx\, dy\; I_P(x, y, z=0, \tau) \exp - \{\beta_{eff} I_L(x, y, z=0, \tau)\}. \tag{3}$$

This expression clearly demonstrates the importance of the spatial and temporal overlap of the laser pulses in the measurement of β.

Similarly to Ref. 10, we define $\rho(I_L)$, the ratio between the transmitted energies of the probe beams through two different samples A and B for identical laser pulses:

$$\rho = \frac{E_T^A}{E_T^B} = K \frac{\exp\{-\alpha_P^A d^A\} \iiint I_P \exp\{-\beta_{eff}^A I_L\}\, d\tau\, dx\, dy}{\exp\{-\alpha_P^B d^B\} \iiint I_P \exp\{-\beta_{eff}^B I_L\}\, d\tau\, dx\, dy} \tag{4}$$

where K is a constant independent of the laser intensity. Note that ρ is a complicated function of I_L and the beam overlap. If the strong laser beam is attenuated in sample A by a filter of transmission F, the factor I_L in the numerator of Eq. (4) should be replaced by $F \cdot I_L$. It is clear that when F obeys the relation

$$F = \beta_{eff}^B / \beta_{eff}^A, \tag{5}$$

the two integrands in Eq. (4) are identical and the ratio ρ is independent

of I_L and the characteristics of the beam overlap. Therefore, since F can be found experimentally by checking the dependence of ρ on I_L, the ratio $\beta_{eff}^B/\beta_{eff}^A$ can be evaluated.

Experiment and Results

The TPA measurements reported here were calibrated using the 2855 cm^{-1} mode of cyclohexane. In Fig. 1 we illustrate our measurement of the inverse Raman absorption cross section of cyclohexane in the region $3000 > \omega_P - \omega_L > 2800$ cm^{-1}. This measurement was done by measuring the attenuation of the variable frequency dye laser probe beam[3, 18, 19] for a normalized intensity of the strong Ruby laser beam. With the narrow linewidth lasers used, the measured spectrum of β_{eff} fits quite well a measurement of the spontaneous Raman scattering which is also presented in Fig. 1. The coincidence between the two spectra is a good check for the reliability of the experimental system.

The absolute Raman cross section of the 2855 cm^{-1} mode of cyclohexane measured in the blue (λ_L = 4880 Å) and reported by Colles and Griffiths[20] is used for calculating $\chi^{(3)}(-\omega_P, \omega_P, \omega_L, -\omega_L)$ using the relationship[14]

$$\chi^{(3)}(-\omega_s, \omega_s, \omega_L, -\omega_L) \propto \frac{1}{\omega_s^3 \omega_L} \frac{d\sigma}{d\Omega} \tag{6}$$

No correction for the small dispersion of $\chi^{(3)}$ was introduced in the calculation of the inverse Raman absorption coefficient, β, from $\chi^{(3)}$. The cross section measurements in Ref. 20 are based on the Raman cross section of the 992 cm^{-1} mode of benzene reported by Skinner and

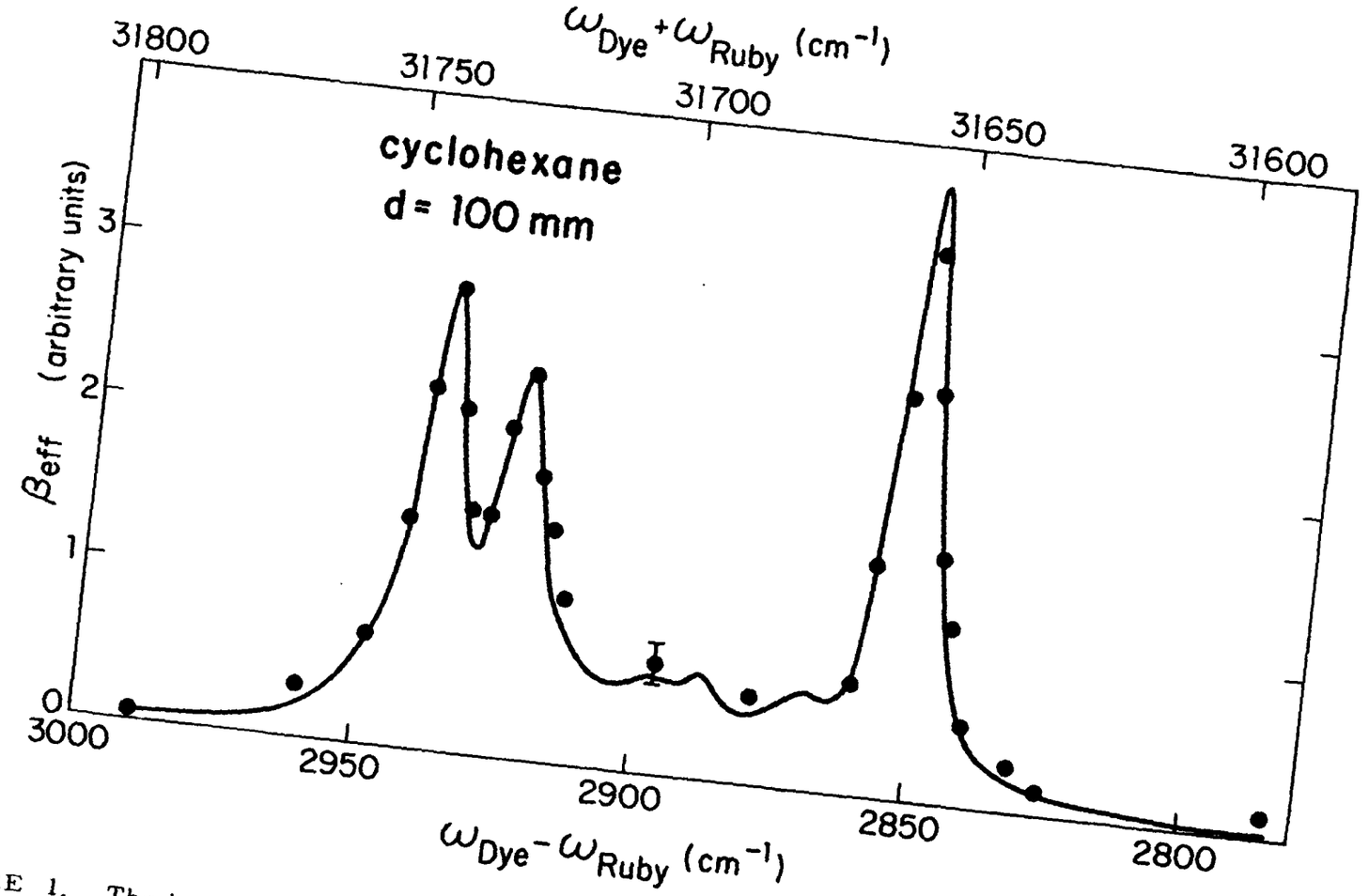

FIGURE 1. The inverse Raman absorption coefficient for parallel probe and laser polarizations vs. $\omega_P - \omega_L$ in a 10 cm cyclohexane cell (points), and the corresponding spontaneous Raman spectrum measured with a 5145 Å laser and 0.4 cm^{-1} spectrometer slits (solid line).

Nilsen.[21] The latter cross section is slightly larger than the one reported by Kato and Takuma.[22] Therefore, the value of β for cyclohexane given here ($\beta = 0.0019$ cm/MW) may be somewhat high. Considering also experimental reproducibility, an uncertainty of about $\pm 20\%$ for the cyclohexane inverse Raman absorption coefficient, β, seems to be reasonable.

The TPA measurements were done using a two-channel normalization technique[10] and the conventional TPA technique.[3,18,19] The experimental setup for the two-channel normalization measurements is shown in Fig. 2. A multimode Ruby laser is used as a source for the strong beam at ω_L and for pumping (after doubling the frequency) a visible dye laser (ω_P). An intracavity telescope in the dye laser is used for narrowing the output below 0.5 Å.[23] The beams of the Ruby and the dye laser are combined by a dichroic-mirror (DM). A glan prism (GS) splits the colinear beams into the cyclohexane cell (S_A) and the examined sample (S_B). After filtration by the cutoff filters (F_i), the two probe beams are detected by two HP 5082-4220 diodes. A plate of ground glass (G) is inserted in front of each diode in order to minimize the effect of the nonuniformity of the laser beam and the diode's active area. The signals are amplified, digitized and punched on a tape which is later analyzed by a computer.[9] The relative intensity of the Ruby laser beam in the samples (i.e., the value of F) may be varied by rotating the double Fresnel prism (DFP) used as a half-wave plate. For a given value of F the ratio $\rho(I_L)$ is measured for different Ruby intensities which are obtained by inserting filters (VA) in the Ruby beam. An iris in front of the splitting prism GS is a critical component in the TPA measurement. By proper setting of this iris the

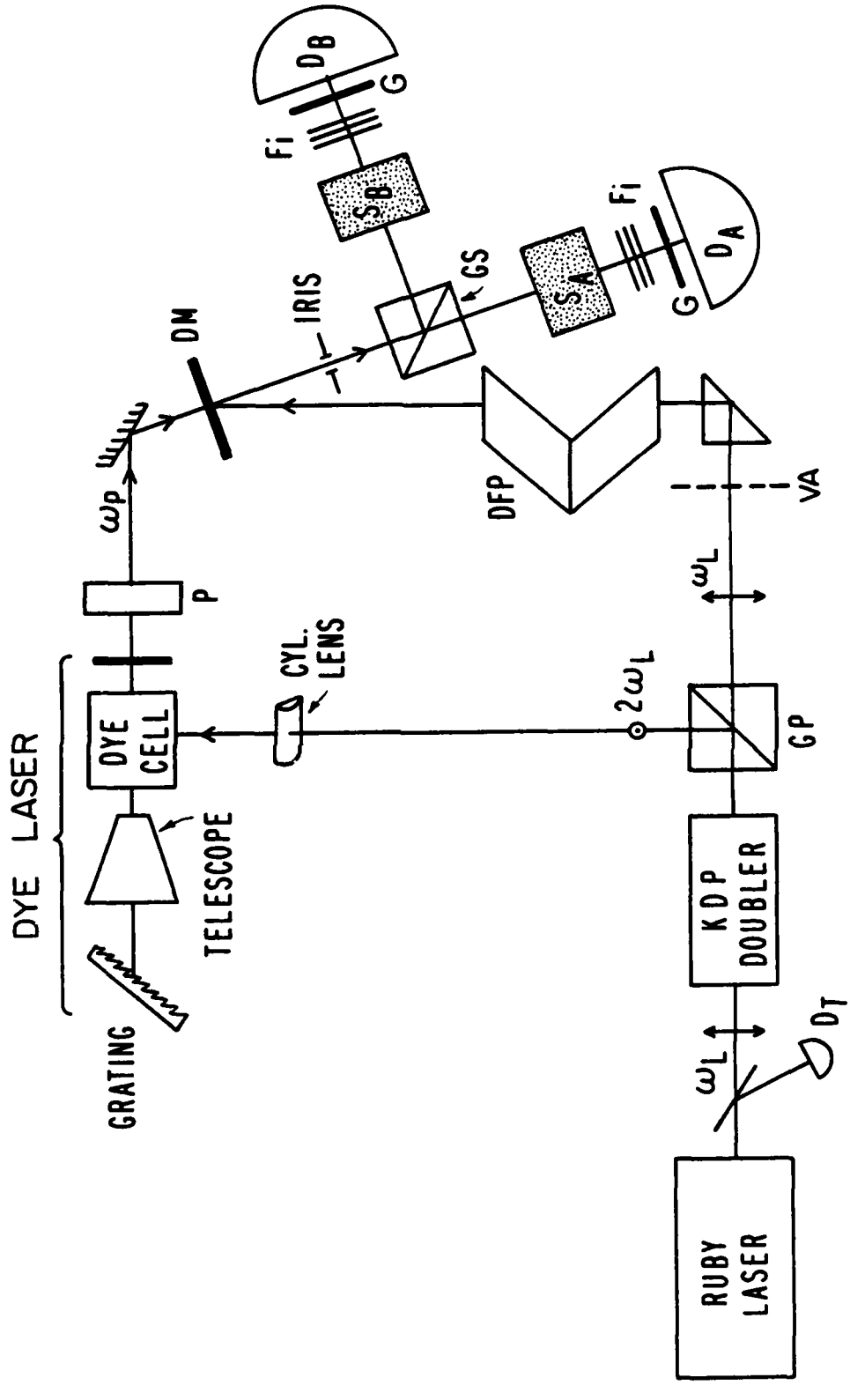

FIGURE 2. The two-channel normalization experimental setup. GP and GS are glan prisms, DFP is a double Fresnel rhomb used as a half wave plate, P is a polarizer with polarization axis at 45° to the vertical, DM is a dichroic mirror, S_A and S_B are the cyclohexane cell and the examined sample, respectively, F_i are cutoff filters, VA is a variable filter, G are ground glass plates, and D_A and D_B are photodiodes with the attached electronics.

overlap integral [Eq. (3)] is maximized.

Fig. 3a shows our results for ρ for CdS/cyclohexane and for CdS/TiO_2. It is seen from the figure that the appropriate values of F for which ρ is independent of I_L are $2.2 < F < 2.56$ and $F \cong 1.4$ for CdS/C_6H_{12} and CdS/TiO_2, respectively. Using Eq. (5) and the linear data of the samples given in Table I, we obtain the values $\beta_{CdS} = .056 \pm .006$ cm/MW and $\beta_{CdS}/\beta_{TiO_2} \cong 2.4$. In a similar way we normalized β of $SrTiO_3$ vs. cyclohexane, $\beta_{SrTiO_3} = .003 \pm .001$ cm/MW.

Using the conventional TPA technique we measured the TPA coefficients of CdS, TiO_2, and GaP relative to the inverse Raman cross section of cyclohexane. The TPA coefficients were obtained by comparing the transmission of the samples at ω_p for different values of I_L. In order to minimize the drift in the experimental conditions, the samples were mounted on a special holder which allowed us to switch samples rapidly. The results of this measurement are shown in Fig. 3b and are tabulated in the fifth column of Table I. For comparison the results of the two-channel normalization measurements are listed in the fourth column of this table. The error bars in Fig. 3 represent the standard deviation of ρ and β_{eff}. The uncertainty in the data points for cyclohexane and TiO_2 shown in Fig. 3b are relatively small because of the large number of laser shots ($\sim$50) averaged at each of these data points.

The value $\beta_{CdS} = .071 \pm .015$ cm/MW and the ratio $\beta_{CdS}/\beta_{TiO_2} = 2.6 \pm .6$ obtained by the conventional TPA technique fits very well the results of the two-channel normalization measurement. The uncertainty in the former measurement is, of course, larger than that of the two-channel experiment.

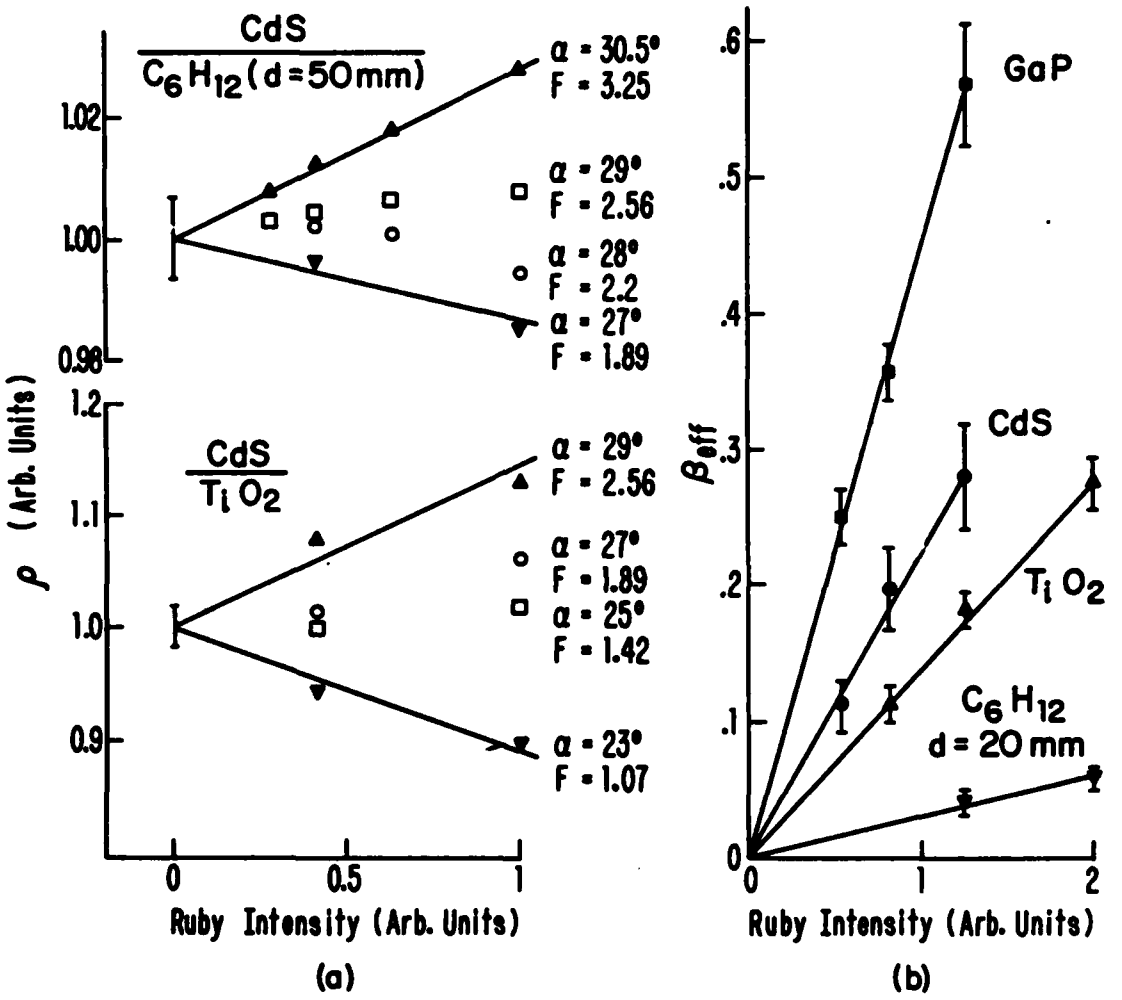

FIGURE 3. a) ρ, the ratio between the transmitted energies in the samples CdS/cyclohexane and CdS/TiO_2 vs. Ruby laser intensity. Each value of F corresponds to a setting angle α of the DFP.

b) β_{eff} vs. Ruby intensity, as we measured by the conventional TPA technique. Each data point represents the average of $\sim$ 10 laser shots except the TiO_2 and cyclohexane with $\sim$50 shots.

TABLE I

	α[a] (cm^{-1})	d (cm)	Reflectivity[b] (%)	β[c] (cm/MW)	β[d] (cm/MW)	Crystal Orientation[f]
CdS	0.06	0.47	17	0.056±0.006	0.071±0.015	$\underline{E} \parallel [1,1,0]$; $\hat{\underline{k}} \parallel [0,0,1]$
GaP	1.45	0.4	28		0.25 ±0.07	$\underline{E} \parallel [1,1,1]$; $\hat{\underline{k}} \perp [0,1,1]$
TiO_2	0.07	0.9	23	0.023±0.004	0.027±0.006	$\underline{E} \parallel [0,0,1]$; $\hat{\underline{k}} \parallel [1,0,0]$
$SrTiO_3$	0.30	0.8	16	0.003±0.001		$\underline{E} \parallel [1,-1,0]$; $\hat{\underline{k}} \parallel [0,0,1]$
Cyclo-hexane	<0.01		4	0.0019[e]	0.0019[e]	Liquid Phase[g]

[a] Absorption constant at the Ruby laser wavelength 6943 Å, measured in a Cary 14 spectrophotometer.

[b] Calculated from index of refraction data.

[c] Our results using the two-channel normalization measurements presented in Fig. 3a.

[d] Our results using the conventional TPA measurements [Fig. 3b].

[e] Based on the data of Ref. 20, see text.

[f] $\underline{E}$ represents the lasers' electric field and $\hat{\underline{k}}$ is the lasers' propagation direction.

Our measured value for β_{zz} of TiO_2 at $\omega_L + \omega_P = 31660\ cm^{-1}$ is about 7 times larger than the value $\beta_{zz} = .0034$ cm/MW obtained by Waff and Park[24] (who used a Nd-glass laser and flash lamp) at the same two-photon energy, and about 3 times larger than $\beta_{xx} = .0065$ cm/MW, obtained by Penzkofer and Falkenstein[25] at $2\omega = 31950\ cm^{-1}$ using a picosecond laser source. (β_{xx} and β_{zz} represent the TPA coefficient for linearly polarized photons, polarized along the x axis and the z axis of the crystal, respectively). No TPA data at $\omega_L + \omega_P \sim 32000\ cm^{-1}$ for the other crystals investigated in this work has been published in the literature.

A comparison of our TiO_2 results with those of Refs. 24 and 25 should be carefully made. We note that the most fundamental physical quantity to be compared is $\chi^{(3)}$ and not β, which includes a trivial frequency factor [see Eqs. (1)]. The large deviation of the result of Ref. 24 probably originates from the severe complications which arose in their experiment in the determination of the overlap integral [Eq. (3)]. The deviation of the results of Ref. 25, however, cannot be explained by the different laser frequencies used, by the small difference between the two-photon energies or by the different electric field polarizations used, which according to Ref. 24 result in the ratio $\beta_{zz}/\beta_{xx} = 1.25$. Dispersion in the TPA coefficient which originates from the one-photon denominators in $\chi^{(3)}$ is also unlikely as an explanation for this deviation since the measurements were done with laser frequencies far enough from the band gap (3.75 eV)[24] to insure no resonant behavior.[16] Also, no $[\chi^{(2)}]^2$ contribution to $\chi^{(3)}$,[12,9] a contribution which depends on the beam polarization and propagation vector, is expected in TiO_2 which exhibits inversion symmetry. Two steps sequential one-photon absorption

contributions to β and absorption caused by two-photon generated holes may, however, influence differently the measurements in the nanosecond and picosecond regimes.[4, 7, 26] We conclude, therefore, that the latter effects and the possibility that the laser pulses in Ref. 25 were not well characterized may explain the deviation of their TiO_2 TPA results from ours.

Discussion and Conclusions

The TPA coefficient and the Raman cross section are important material parameters. Accurate values of TPA coefficients and especially their spectral dependence will be useful for stimulating further theoretical calculations of two-photon phenomena. In particular, existing theoretical models of matter such as the "empirical pseudopotential method"[27] may be checked by comparing the theoretical β based on the specific model with the experimental one. We note that one-photon spectroscopy above the material band gap shows surface effects because of the small penetration depth. The TPA measurement, however, reflects in the same spectral region only the bulk properties of the material. Therefore, a comparison of the TPA experimental results with theoretical models is more direct than in the one-photon case. Experimentally, accurate TPA coefficients may be used for the characterization of pulsed laser beams.[25] This may be done by checking the interaction of the strong beam with a probe beam whose parameters are well known (cw dye laser beam, for example) in a NL absorber. The measured value of E_T [see Eq. (3)] may give important information on the spatial and temporal properties of

the strong beam. In particular, absolute peak power values, which are very important in multiphoton processes, may be obtained by this method. Accurate Raman cross sections may be used for measuring average concentrations of molecular species over long atmospheric paths using stimulated Raman gain[19] or inverse Raman loss experiments.

The calibration method described here is very useful for reliable measurements of TPA coefficients. Raman cross sections may also be calibrated by the same method. In this case, inverse Raman absorption as well as stimulated Raman gain may be utilized in the measurement. The use of a probe beam in the absorption measurement has an advantage over the standard one-beam TPA methods. In the one-beam case, any small loss in the laser beam caused by other NL processes may strongly influence the measured cross section. Such perturbations which influence the strong laser beam have only a minor effect on the probe beam.

In conclusion, we have described a technique which allows simple measurement of TPA coefficient and Raman cross section, relative to known inverse Raman cross sections. The use of the two-channel normalization experiment enables one to eliminate the dependence of the NL absorption on the laser intensity, thereby removing the usual problems associated with absolute intensity measurements. Additionally, this normalization alleviates sources of errors due to irreproducible laser pulse spatial and temporal profile, allowing the measurement to be made with simple uncontrolled lasers.

REFERENCES

1. The TPA selection rules are comprehensively reviewed by W. M. McClain, J. Chem. Phys. 55, 2789 (1971).
2. D. Fröhlich, Comments on Solid State Phys. 4, 179 (1972); J. M. Worlock, in Laser Handbook, edited by F. T. Arecchi and E. O. Schulz-DuBois (North Holland, Amsterdam, 1972); Vol. I, p. 1323; V. I. Bredikhin, M. D. Galanin and V. N. Genkin, Usp. Fiz. Nauk. 110, 3 (1973) [Sov. Phys.-Usp. 16, 299 (1973)]; H. Mahr, in Quantum Electronics, ed. H. Rabin and C. L. Tang (Academic Press, New York, 1975), Vol. I, p. 285.
3. R. L. Swofford and W. M. McClain, Rev. Sci. Instrum. 46, 246 (1975).
4. J. H. Bechtel and W. L. Smith, Phys. Rev. B13, 3515 (1976).
5. J. P. Hermann and J. Ducuing, Phys. Rev. A5, 2557 (1972).
6. M. D. Levenson and N. Bloembergen, J. Chem. Phys. 60, 1323 (1974); Phys. Rev. B10, 4447 (1974).
7. R. T. Lynch, Jr. and Haim Lotem, J. Chem. Phys. (1977).
8. H. Lotem and R. T. Lynch, Jr., Phys. Rev. Lett. 37, 334 (1976).
9. S. D. Kramer and N. Bloembergen, Phys. Rev. B15, 4654 (1976).
10. H. Lotem, J. H. Bechtel and W. L. Smith, Appl. Phys. Lett. 28, 389 (1976).
11. A similar normalization measurement of the NL refractive index is reported by M. J. Moran, Chiao-Yao She and R. L. Carman, IEEE J. Quant. Electron. QE-11, 259 (1975).

12. Chr. Flytzanis and N. Bloembergen, in Progress in Quantum Electronics, eds. J. H. Sanders and S. Stenholm (Pergamon Press, New York, 1976). The equivalent behavior of the TPA and the Raman contributions to $\chi^{(3)}$ is clearly discussed in this reference.

13. W. J. Jones and B. P. Stoicheff, Phys. Rev. Lett. 13, 657 (1964); W. Werncke, J. Klein, A. Lau, K. Lenz and G. Hunsalz, Opt. Comm. 11, 159 (1974); A. Lau, W. Werncke, M. Pfeiffer, K. Lenz, and H. J. Weigman, Kvant. Electron. 3, 739 (1976) [Sov. J. Quant. Electron. 6, 402 (1976)].

14. N. Bloembergen, Nonlinear Optics, (Benjamin, New York, 1965).

15. A. Owyoung, Opt. Comm. 26, 266 (1976).

16. H. Lotem, R. T. Lynch, Jr. and N. Bloembergen, Phys. Rev. A14, 1748 (1976).

17. N. Bloembergen, Am. J. Phys. 35, 989 (1967).

18. R. G. Stafford and M. Sondergeld, Phys. Rev. B10, 3471 (1974).

19. B. E. Kincaid and J. R. Fontana, Appl. Phys. Lett. 28, 12 (1976).

20. M. J. Colles and J. E. Griffiths, J. Chem. Phys. 56, 3384 (1972).

21. J. G. Skinner and W. G. Nilsen, J. Opt. Soc. Am. 58, 113 (1968).

22. Y. Kato and H. Takuma, J. Chem. Phys. 54, 5398 (1971).

23. T. W. Hänsch, Appl. Opt. 11, 895 (1972).

24. H. S. Waff and K. Park, Phys. Lett. 32A, 109 (1970)

25. A. Penzkofer and W. Falkenstein, Opt. Comm. 17, 1 (1976).

26. J. F. Reintjes and J. C. McGrodyy, Phys. Rev. Lett. 30, 901 (1973).

27. M. L. Cohen and T. Bergstresser, Phys. Rev. 141, 789 (1966); G. Koren, Phys. Rev. B11, 802 (1975).

D. NONLINEAR ABSORPTION AND REFLECTION IN InSb DURING SHORT CO_2-LASER PULSES

Nonlinear interactions of light in semiconductors has been studied intensively over the last fifteen years by various authors [1-3]. In the high intensity limit, the material of course breaks down and suffers irreversible damage [4]. In the low intensity limit, a perturbative approach is usually taken whereby the interaction is described as a multiphoton process [5]. It is in the region just below the material breakdown threshold that is of fundamental physical interest and is relatively unexplored experimentally. In this regime, electron-hole generation is unavoidable and the interaction of light with the material is a mixture of intrinsic material interaction and plasma effects.

In this section a study of the behavior of InSb under interaction with high intensity 10.6 μ radiation is described. In the past, experimental studies of plasma behavior were done with picosecond 1.06 μ pulses [6-8]. This is because of the ability to go to high peak power without damaging the crystal since damage thresholds are mostly energy thresholds. We are able to generate 50 psec. CO_2 pulses with ~ 0.5 Mw power and therefore can extend such studies to small band gap materials [9]. In addition to being a pulse shaper and limiter for high power lasers [10], InSb is interesting because of its highly nonparabolic energy bands and associated nonlinearities. Its behavior at high intensities has been studied theoretically by Tzoar and Gersten [11].

Figure 1 shows the transmitted energy of a sample of InSb doped to $n = 6.6 \times 10^{16}$ cm^{-3} versus incident laser intensity. It is seen that the relative transmittance decreases by a factor of four at high intensities.

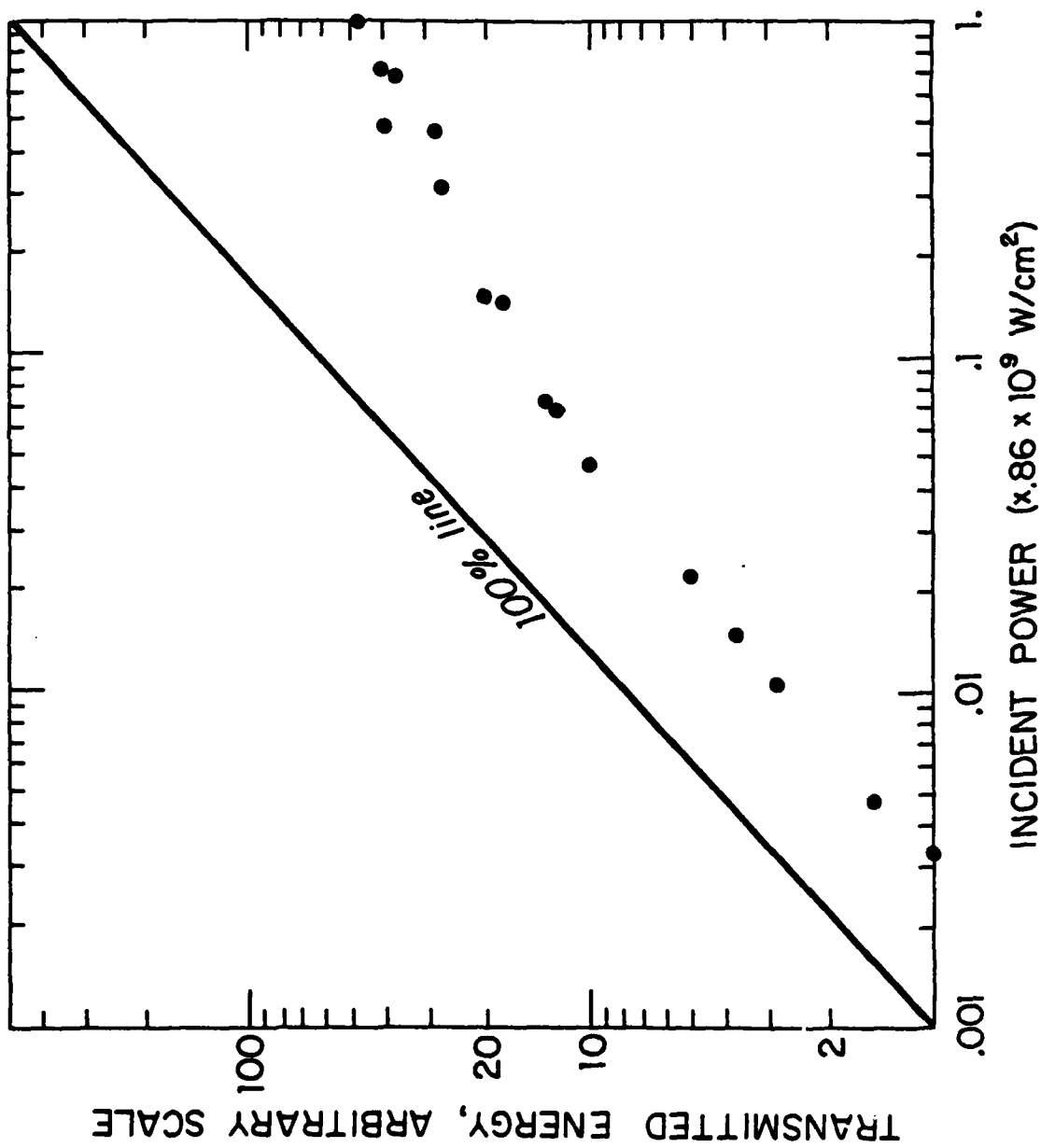

FIGURE 1. Transmitted energy versus incident intensity for $\eta = 6.6 \times 10^{16}$ cm^{-3} sample.

This is probably due to the generation of a critically dense electron-hole plasma rather than by two-photon absorption alone. To confirm this, we made a calculation similar to Bechtel [12] to determine the two-photon absorption coefficient. From our experimental data for the transmittance a value of 9.1 cm/Megawatt was derived, which is a factor of 35 larger than the established value of 0.23 cm/Mw [10, 13]. The reason is that carrier effects cannot be ignored in the calculation. In view of this, it is more advisable to look at the reflectance.

Figure 2 shows the reflectance of a highly doped sample ($n = 1.5 \times 10^{18}$ cm^{-3}) versus intensity. A brewster angle of incidence was used. The reflectivity changes by more than a factor of six. What we actually measured was the integrated transient reflectivity R(t) [14]. The increase in reflectivity is a manifestation of the changing index of refraction due to formation of a plasma. The electron generation mechanism is by multiphoton injection [13, 15].

$$\frac{\partial n}{\partial \tau} = \frac{\alpha I}{\hbar\omega} + \frac{\beta I^2}{2\hbar\omega} - \frac{n}{\tau} - \gamma n(n+n_0)$$

where γ is the radiative recombination rate and τ is the nonradiative recombination time which is mostly due to Auger recombination. α is single photon excitation from intermediate levels and β is the TPA coefficient. The single photon term has been measured by Fossum [13] at $77^{\circ}K$. With their number for α and at our intensity, the first term is four orders of magnitude smaller than the second term. It is expected to be even smaller at high temperature since the intermediate states are all thermally ionized to begin with. The estimated recombination lifetime is 500 nsec. and the nonradiative recombination time is 23 nsec. [10, 13].

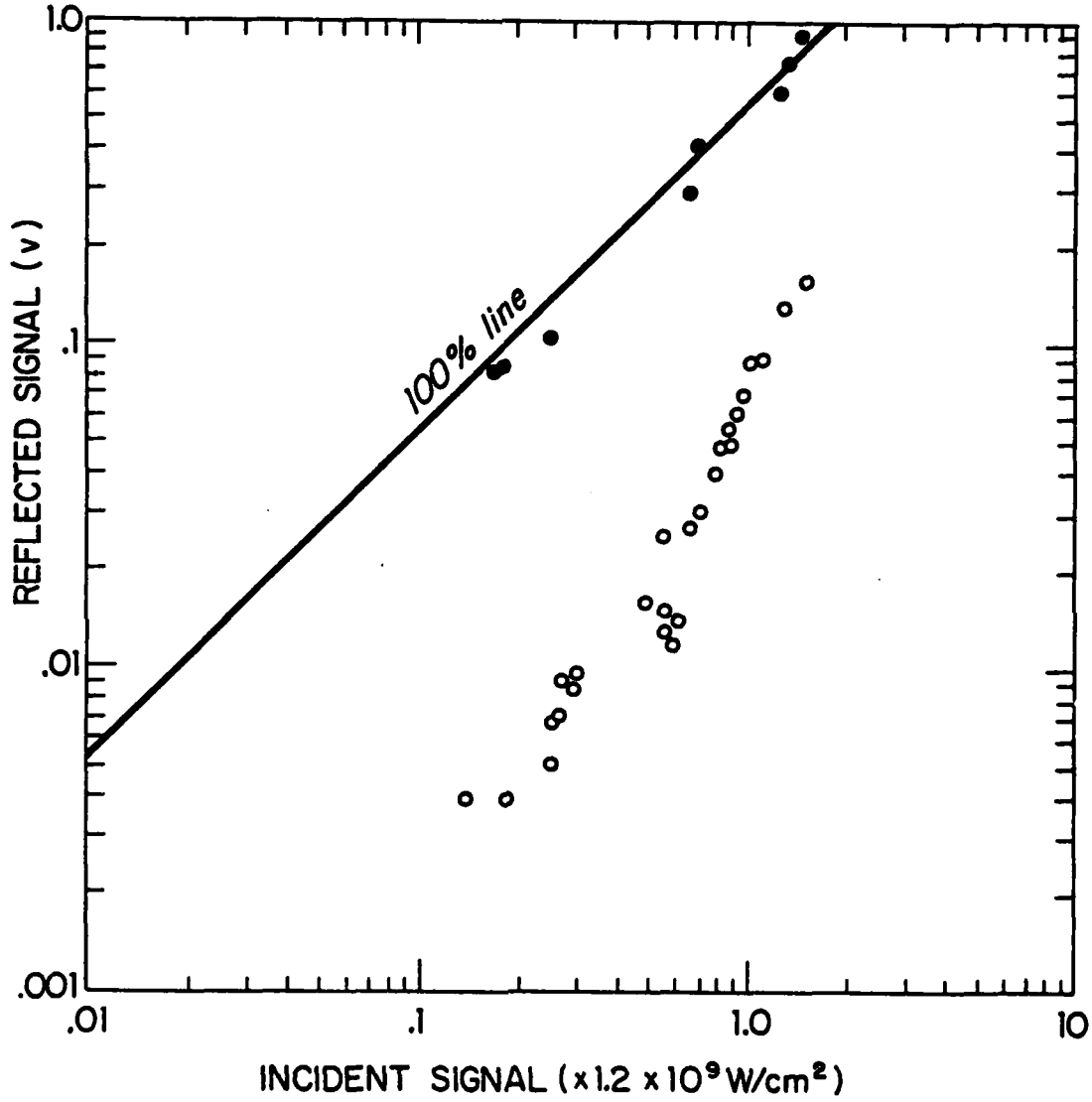

FIGURE 2. Reflected energy versus incident intensity for $\eta = 1.5 \times 10^{18}$ cm^{-3} sample. Black dots: data points for reflection from a polished aluminum mirror. Open dots: data points for sample.

Therefore, recombination is largely nonradiative. Since both times are much larger than the pulsewidth, they can be ignored, and the equation describing plasma generation is simply

$$\frac{\partial n}{\partial \tau} = \beta \frac{I^2}{2\hbar\omega}$$

For small reflectivities in the region of the brewster minimum, it can be shown that

$$R \sim \left(\frac{\partial n}{\partial t}\right)^2 \quad .$$

However, the experimental curve in Figure 2 shows that R is approximately proportional to the intensity, implying that n grows only as the square root of the intensity. This is an indication that our simple model of two photon ionization is not valid at such high intensities. A straightforward Keldysh type calculation [1, 16] shows that the ionization process changes from a multiphoton character to a tunneling character at around $I_{c\tau} = 5.5 \times 10^9$ W/cm^2 for our sample. In the tunneling regime, the rate of carrier generation follows a Keldysh type of equation

$$\frac{\partial n}{\partial t} \propto I^2 (I_{cr}/I)^{3/4} \exp\{-3.9 (I_{cr}/I)^{1/2} (1 - I_{cr}/8I)\}$$

This expression is in rough agreement with the experimental trend. A quantitative calculation should take into account the temporal variation of I during the pulse. The accuracy of the measurement must also be further improved.

References

1. L. V. Keldysh, Zh. Eksp. Fiz. 47, 1945 (1964) [Sov. Phy. Jet-P 20, 1307 (1964)].

2. Man Mohan and S. N. Hague, Phys. Rev. A9, 631 (1974); G. M. Aratyunyan and S. M. Shahinyan, Phys. Stat. Sol. (b) 77, K171 (1976).

3. Howard R. Reiss, Phys. Rev. A1, 803 (1970).

4. W. Lee Smith, J. H. Bechtel and N. Bloembergen, TR No. 665, Division of Engineering and Applied Physics, Harvard University.

5. R. Braunstein and N. Ockman, Phys. Rev. 134, A499 (1964).

6. C. V. Shank and D. H. Auston, Phys. Rev. Lett. 34, 479 (1975).

7. John F. Reintjes and James C. McGroddy, Phys. Rev. Lett. 30, 901 (1973).

8. D. J. Kennedy et al., Phys. Rev. Lett. 32, 419 (1974).

9. H. S. Kwok and E. Yablonovitch, Appl. Phys. Lett. 30, 158 (1977).

10. A. F. Gibson et al., J. Phys. CC: Solid State Phys. 9, 3, 259 (1976).

11. N. Tzoar and J. I. Gersten, Phys. Rev. B12, 1132 (1975).

12. J. H. Bechtel and W. L. Smith, Phys. Rev. 13, 3515 (1976).

13. H. J. Fossum and D. B. Chang, Phys. Rev. 8, 2842 (1973); H. J. Fossum, W. S. Chen, and B. Ancker-Johnson, Phys. Rev. 138, 2857 (1973).

14. S. A. Jamison, A. V. Nurmikko, and H. J. Gerritsen, Appl. Phys. Lett. 29, 64 (1976).

15. R. E. Slusher, W. Giriat and S. R. J. Brueck, Phys. Rev. 183, 758 (1969).

16. S. S. Mitra, L. M. Narducci, R. A. Shatas, Y. F. Tsay and A. Vaidyanathan, Appl. Opt. 14, 3038 (1975).


2-8
DT